Immunosuppressive potential of fowl adenovirus serotype 4

Yujuan Niu,[*,†,1] Qinqin Sun,[†] Yongyong Shi,[*] Yonghe Ding,[*] Zhiqiang Li,[*] Yuanchao Sun,[*] Meihang Li,[*] and Sidang Liu[†,1]

[*] *The Affiliated Hospital of Qingdao University and The Biomedical Sciences Institute of Qingdao University (Qingdao Branch of SJTU Bio-X Institutes), Qingdao University, Qingdao, Shandong Province 266003, China; and* [†] *College of Animal Science and Technology, Shandong Agricultural University, Tai'an, Shandong Province 271018, China*

ABSTRACT Fowl adenovirus serotype 4 (FAdV-4) is the causative agent of hydropericardium syndrome. To clarify the effects of FAdV-4 on immune organs in birds, we conducted a detailed examination of dynamic morphology and damage mechanisms in chickens randomly divided into 4 groups (FAdV-4, vaccination, FAdV-4 plus vaccination, and control). FAdV-4 caused the depletion of lymphocytes and subsequent growth impairment in the thymus and bursa. Chickens infected with FAdV-4 and subjected to vaccination experienced greater inhibition of antibody responses to inactivated vaccines against Newcastle disease and avian influenza virus subtype H9 than uninfected and vaccinated chickens. The mechanisms underlying adenovirus-mediated lymphoid organ damage were further investigated via transferase-mediated dUTP nick-end labeling and apoptotic genes transcription analyses. Notably, lymphocytes apoptosis in lymphoid organs and expression of specific gene transcripts was significantly upregulated after infection ($P < 0.05$). Furthermore, increased expression of interleukin (IL)-6, IL-8, and tumor necrosis factor (TNF)-α mRNA was observed ($P < 0.05$), compared to the control group. Our collective findings suggested that FAdV-4 caused structural and functional damage of immune organs via apoptosis along with induction of a severe inflammatory response.

Key words: apoptosis, FAdV-4, immune organs, immunosuppression, inflammatory response

2019 Poultry Science 98:3514–3522
http://dx.doi.org/10.3382/ps/pez179

INTRODUCTION

Hydropericardium syndrome (**HPS**), prevalent in commercial chicken farms in China since mid-2015, causes high mortality in diseased chickens resulting in tremendous economic losses to poultry farmers (Li et al., 2016; Niu et al., 2016; Ruan et al., 2018). Fowl adenovirus serotype 4 (**FAdV-4**) is the causative agent of HPS (Lobanov et al., 2000; Schachner et al., 2014; Li et al., 2016). At present, HPS is distinguished by accumulation of a clear, straw-colored fluid in the pericardial sac as well as acute and hemorrhagic hepatitis (Lobanov et al., 2000; Schachner et al., 2014). The majority of previous studies have thus focused on the pathogenesis of FAdV-4 in heart and liver (Niu et al., 2018a,b). In the poultry industry, co-infections with FAdVs and other pathogens are detected regularly (Ojkic et al., 2008; Choi et al., 2012; Kaján et al., 2013). However, limited evidence on the immunosuppressive activity of FAdV-4 in chickens is available in the literature. In natural HPS cases, necrosis of lymphocytes has been observed in chicken immune organs. In the current study, we conducted a detailed examination of the dynamic morphology and damage mechanisms with a view to determining the effects of FAdV-4 on immune organs.

Several human adenoviruses are reported to trigger apoptosis and a severe inflammatory response in host cells (Jiang et al., 2011; Rodriguez-Rocha et al., 2011; Radke et al., 2014). Apoptosis is a physiological and pathological phenomenon. Excessive apoptosis can lead to physical dysfunction. Infection with pathogenic viruses can lead to activation of the apoptotic machinery in infected cells (Levine, 2005; Radke et al., 2014). Viruses additionally use apoptosis to escape antiviral host activity and maintain survival and replication (Zhong et al., 2012; Pruijssers et al., 2013). Viral infections are recognized initially via Rig-I-like or Toll-like receptors (Kawai and Akira, 2008). Signaling through these receptors elicits the release of numerous cytokines, including IL-6, IL-8, and TNF-α (Manicassamy and Pulendran, 2009), which, in turn, triggers an inflammatory response that recruits antiviral cells, such as monocytes, macrophages, and lymphocytes (Barlan et al., 2011). However, excessive inflammation can also damage the tissue.

Received January 21, 2019.
Accepted March 15, 2019.
[1]Corresponding author: yujuanniu@163.com (YN); liusid@sdu.edu.cn (SL)

Table 1. The primers used in the present study

Gene symbol	Primer sequence	Products size (bp)
Bax	F: 5′-ATGGATGCCTGTCTGTCCTGTTC-3′ R: 5′-GCAGAGCAGTCCAAAGACACTGA-3′	106
Bcl2	F: 5′-CAGAGGGACTTCGCCCAGAT-3′ R: 5′-ACATCACGCCGCCGAACT-3′	148
P53	F: 5′-CAGAGGGACTTCGCCCAGAT-3′ R: 5′-ACATCACGCCGCCGAACT-3′	120
Caspase3	F: 5′-ACTCTGGAA ATTCTGCCTGATGACA-3′ R: 5′-CATCTGCATCCGTGCCTGA-3′	129
Il6	F: 5′-CCAGAAATCCCTCCTCGCCAATC-3′ R: 5′-GCCCTCACGGTCTTCTCCATAAAC-3′	111
Il8	F: 5′-GCTCTGTCGCAAGGTAGGA-3′ R: 5′-TGGCGTCAGCTTCACATCT-3′	117
Tnfα	F: 5′-TACTCAGGACAGCCTATGCCAACA-3′ R: 5′-CACCACACGACAGCCAAGTCAA-3′	178

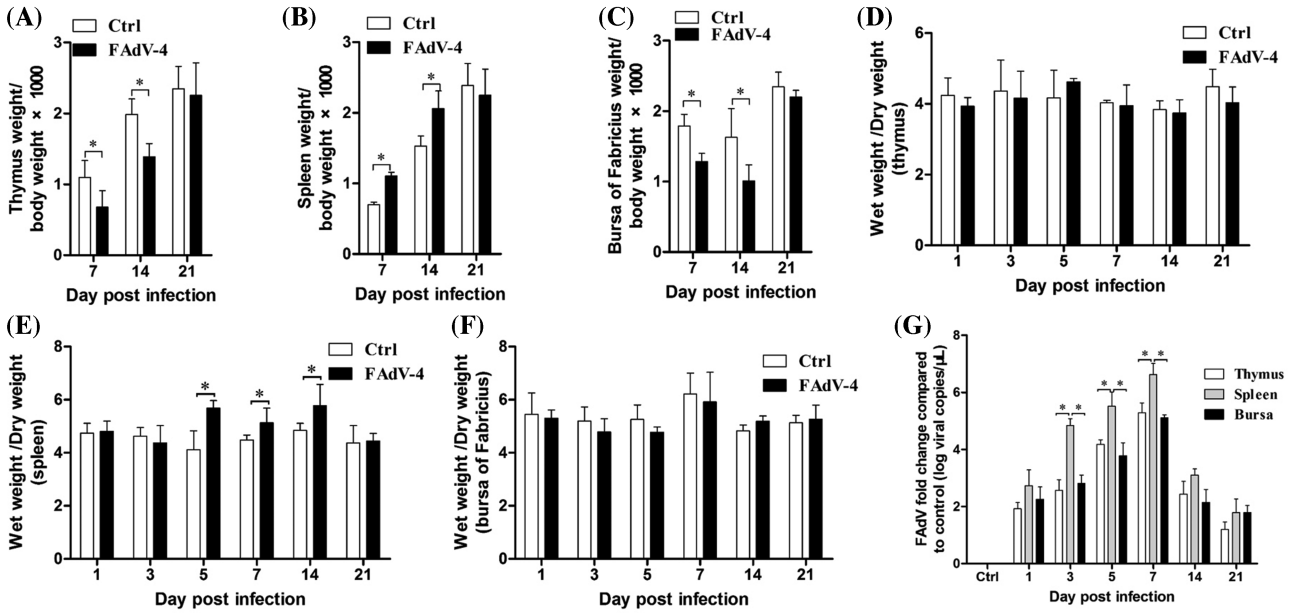

Figure 1. The clinical indices of immune organs after inoculation with fowl adenovirus serotype 4. **(A–C)** The mean relative organ weights for thymus, spleen, and bursa of infected birds compared with the control group at 7, 14, 21 days post-infection (dpi). **(D–F)** The wet-to-dry weight ratio in thymus, spleen, and bursa of infected birds compared with the control group at 7, 14, 21 dpi. **(G)** Viral load in thymus, spleen, and bursa. Data are expressed as mean ± SD ($n = 5$ chicken per group). Asterisks indicate significant differences compared with the controls ($P < 0.05$, by 1-way ANOVA).

The present study was undertaken to assess the lymphoid organ tropism of FAdV-4 and extent of suppression of the humoral immune response. We further determined whether the mechanism underlying FAdV-4-induced immune organ damage involved apoptosis and an inflammatory response. Our collective results contribute to current knowledge on the pathological mechanisms of FAdV-4-induced disease.

MATERIALS AND METHODS

Ethics Statement

This study was approved by the Animal Care and Use Committee of Shandong Agricultural University (permit number: SDAUA-2015-003) and performed in accordance with the "Guidelines for Experimental Animals" of the Ministry of Science and Technology (Beijing, China). All the chickens were cared for in accordance with the humane procedures.

Virus

The FAdV-4 strain (SDDM-4/15) used in the present study was isolated from a liver sample of a broiler chicken during a recent HPS outbreak in China (Niu et al., 2016). The virus was cultured in the chicken hepatocellular carcinoma cell line (LMH) (ATCC CRL-2117) that was obtained from the American Type Culture Collection (Manassas, VA, USA). LMH cells were grown in Waymouth's MB 752/1 (M&C, Beijing, China) containing 10% fetal bovine serum (BI, Israel) at 37°C in 5% CO_2. Supernatants and cells were harvested after 60 h incubation, and determination of the median tissue culture infectious doses ($TCID_{50}$) of the FAdV-4 in LMH was conducted. A viral titer of 10^7

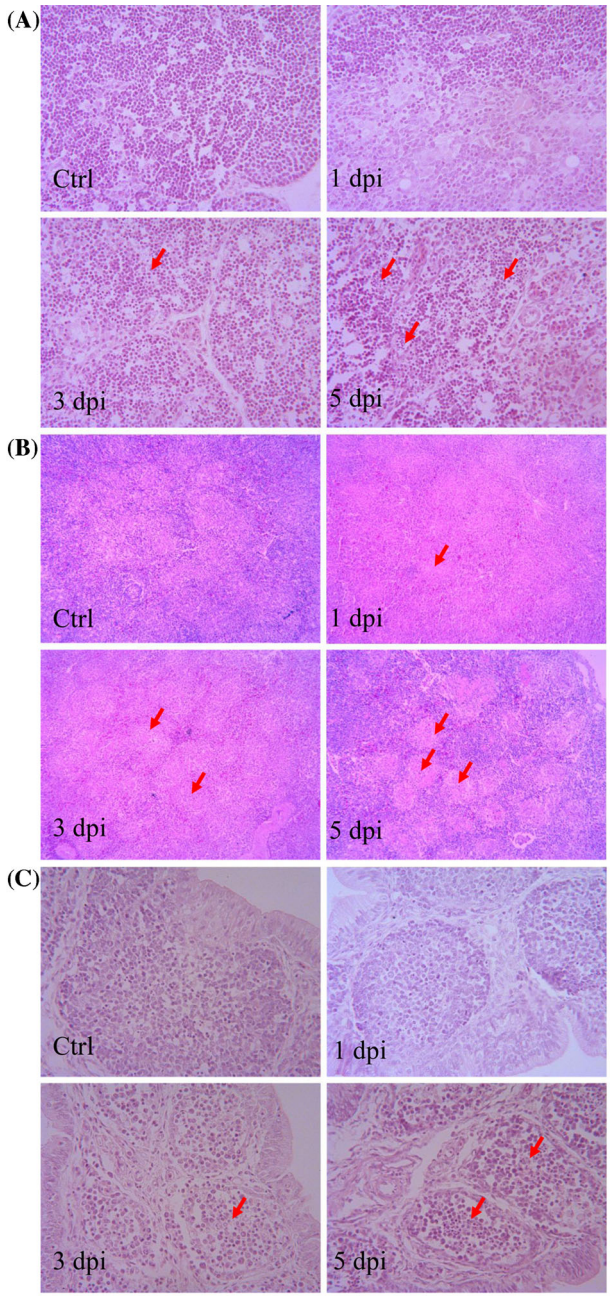

Figure 2. Histopathology of immune organs. Lymphocytes depletion and necrosis of thymus **(A)**, spleen **(B)**, and bursa **(C)** in a time-dependent manner. The red arrow indicates the necrotic area of lymphocytes.

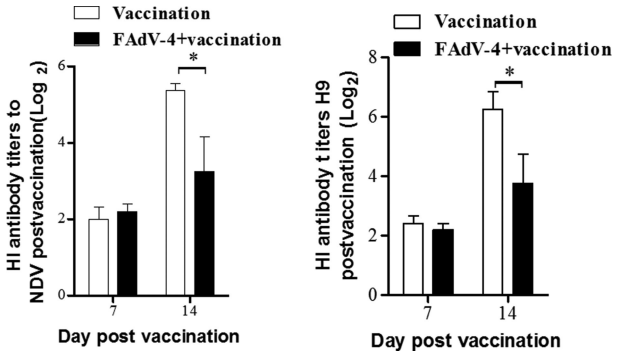

Figure 3. Influence of fowl adenovirus serotype 4 (FAdV-4) infection on hemagglutination inhibition antibody titers against Newcastle disease (NDV) and AIV-H9 post-vaccination in specific-pathogen-free chickens (Log2). The antibody titers of NDV and AIV-H9 in FAdV-4 plus vaccination group were significantly weaker in vaccination group at 14 d post-vaccination. Data are expressed as mean ± SD ($n = 10$ chicken per group). Asterisks indicate significant differences compared with the controls ($P < 0.05$, by 1-way ANOVA).

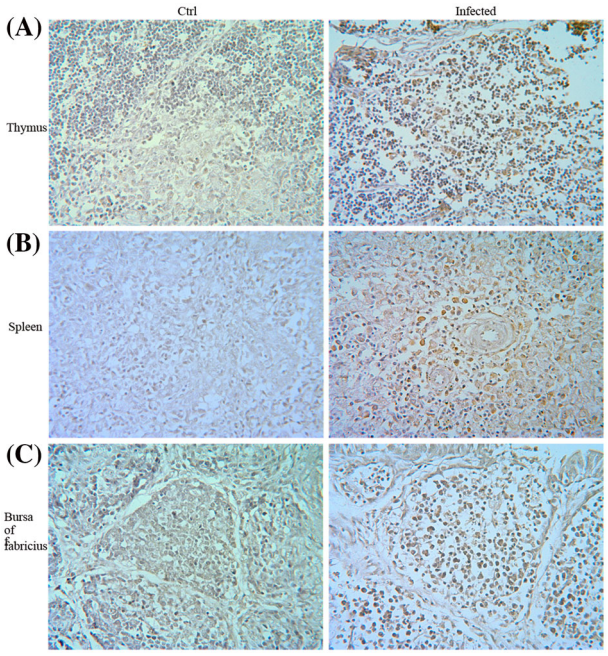

Figure 4. Fowl adenovirus serotype 4 induces apoptosis in the thymus, spleen, and bursa. Transferase-mediated dUTP nick-end labeling staining (digoxigenin labeling, brown spots) at 5 d post-infection (original magnification, 100×).

tissue culture infective dose in 0.2 mL was used to inoculate chicks.

Animal Trial

One hundred and thirty 7-day-old specific-pathogen-free (**SPF**) chickens were divided randomly into 4 treatment groups (30 in the control, 70 in the FAdV-4, 10 in the vaccination, and 20 in the FAdV-4 plus vaccination groups). Chickens were housed in separated isolators receiving filtered positive pressure air. Birds in the FAdV-4 and FAdV-4 plus vaccination groups were inoculated subcutaneously with 0.2 mL SDDM-4/15 at 7 d of age while those in the control group were left uninoculated. At 14 d of age, birds in the vaccination and FAdV-4 plus vaccination groups were injected subcutaneously with inactivated vaccine against Newcastle disease (**NDV**) and avian influenza virus subtype H9 (AIV-H9) (Qilu Animal Health Products Co., Ltd., Jinan, China). To determine the immunosuppressive effect of the virus on antibody response to vaccination, 10 serum samples collected from live chickens of each group (vaccination and FAdV-4 plus vaccination) on days 7 and 14 post-vaccination were used to measure the hemagglutination inhibition (**HI**) antibody titers against NDV and AIV-H9 following standard procedures.

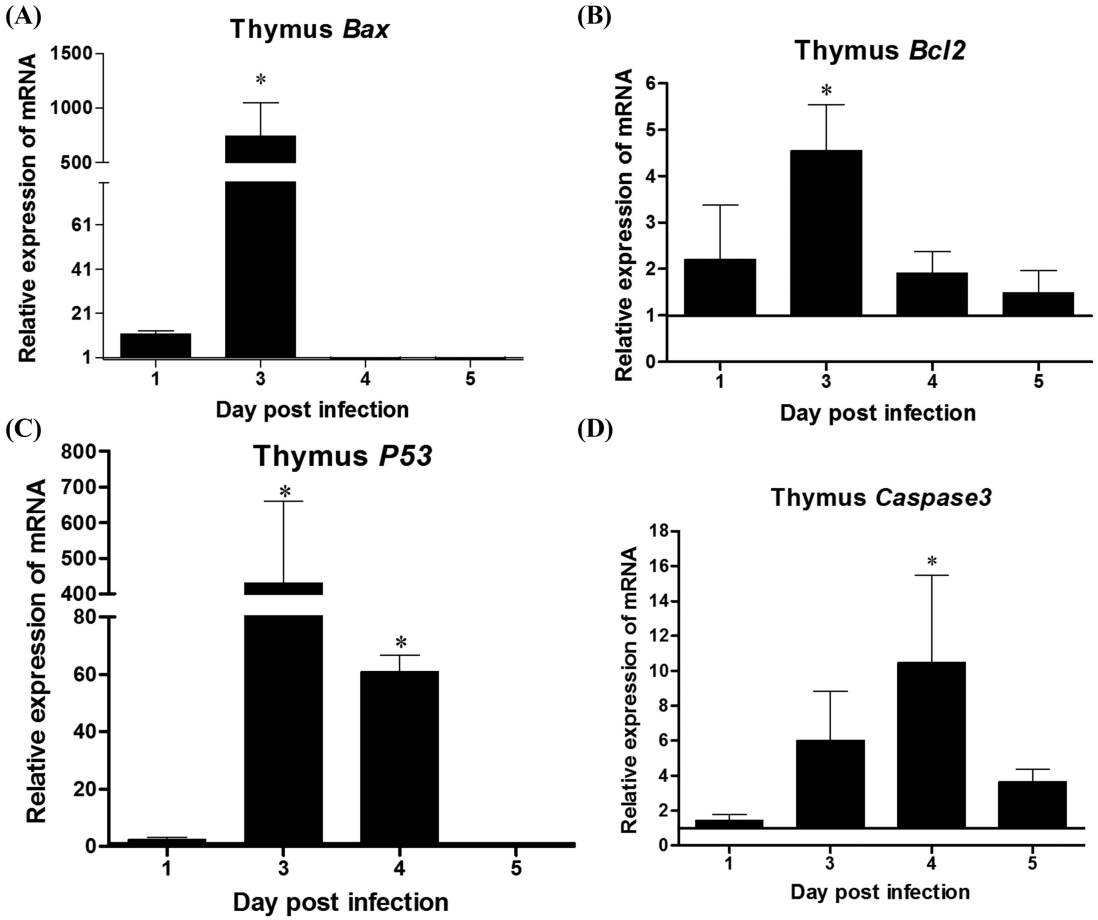

Figure 5. Expression profiles of apoptosis-related genes in the thymus at 1, 3, 4, and 5 d post-infection with fowl adenovirus serotype 4 infection. (A) *Bax,* (B) *Bcl2,* (C) *P53*, (D) *Caspase3* mRNA levels. The y axis represents the fold change in target gene expression in thymus compared with that of the control and the above line ($y = 1$) on the x axis represents the control. Data are expressed as mean ± SD ($n = 5$ chicken per group). Asterisks indicate significant differences ($P < 0.05$, by 1-way ANOVA).

Dead chickens in the FAdV-4 and FAdV-4 plus vaccination groups were not considered.

Postmortem and Measuring the Weight of Immune Organs

To determine the dynamic changes in histopathology in major lymphoid organs, 5 chickens from control and FAdV-4 groups were bled and euthanized, and the spleen, bursa, and thymus collected at 1, 3, 5, 7, 14, and 21 days post-infection (**dpi**). Body weights of all SPF birds from the 2 groups were measured and individual weights recorded. Spleen, thymus, and bursa from each bird were weighed after collection, and their relative weights to the whole body were determined using the formula: organ weight (g) = organ wt/body wt (g) × 1000. Sample tissues were additionally collected to analyze the ratio of wet to dry weight. Sample tissues were further fixed in 4% neutral-buffered formalin, embedded in paraffin blocks, and cut into 4 μm sections, which were stained with hematoxylin and eosin and examined under a light microscope for lesions associated with FAdV-4 infection.

In Situ Apoptosis Detection

The in situ labeling of immune organs was performed using a terminal deoxynucleotidyl transferase-mediated dUTP nick-end labeling (**TUNEL**) assay with commercial kits (BOSTER, Wuhan, China).

Viral DNA Detection in Tissues

At 1, 3, 5, 7, 14, and 21 dpi, 5 chickens from control and FAdV-4 groups were collected to determine tissue distribution of the virus by qPCR. Total DNA was extracted from 200 μL of the homogenized tissue samples with Tris-phenol (Solarbio, Beijing, China) according to manufacturer's instructions. The absolute FAdV-4 genomic load in tissues was quantified using the following primers: the FAdV-4 forward primer, 5′–GACGGCGGCGCAGGTGACGAAGATT–3′, and the FAdV-4 reverse primer, 5′–TGAGACTTGGCGAA GCGACCGAGCA–3′. A standard curve was prepared over a 10-fold range of dilutions with comparable reaction efficiencies to estimate the viral copy numbers from the sample cycle threshold values. The standard sample was a plasmid containing a 126-bp fragment of

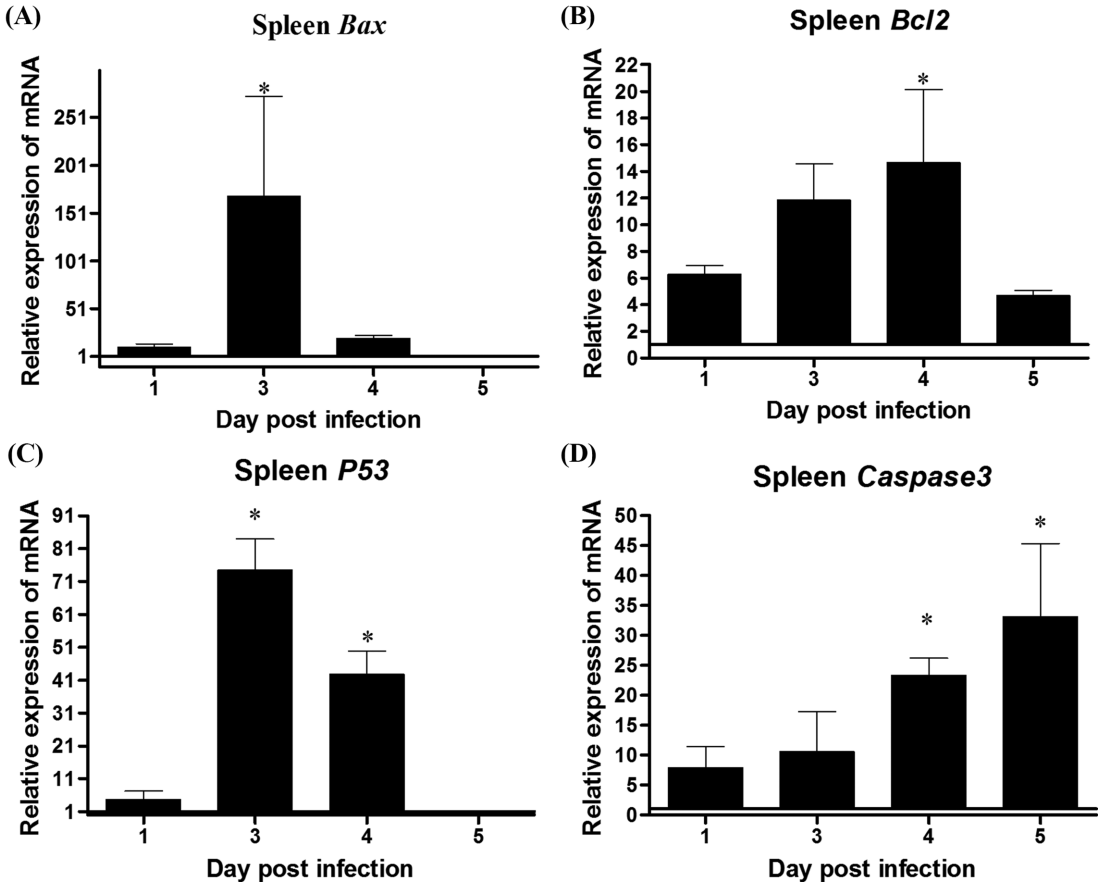

Figure 6. Expression profiles of apoptosis-related genes in spleen at 1, 3, 4, and 5 d post-infection with fowl adenovirus serotype 4 infection. (A) *Bax,* (B) *Bcl2,* (C) *P53,* (D) *Caspase3* mRNA levels. The y axis represents the fold change in target gene expression in spleen compared with that of the control and the above line ($y = 1$) on the x axis represents the control. Data are expressed as mean ± SD ($n = 5$ chicken per group). Asterisks indicate significant differences ($P < 0.05$, by 1-way ANOVA).

FAdV-4 that was amplified with the primers pair and then cloned into the pCAGGS vector (Invitrogen Corporation, Carlsbad, CA). Seven 10-fold serial dilutions of the plasmid were performed, which produced a range of 1.42×10^2 to 1.42×10^9 plasmid copies per reaction.

Total RNA Extraction and Real-time qPCR

Total RNA was extracted from the thymus, spleen, and bursa with TRIzol reagent (Takara, Dalian, China). First-strand cDNA was synthesized from 1 μg total RNA using the Transcriptor First Strand cDNA Synthesis Kit (Roche). All products were stored at –20°C prior to further use. Real-time qPCR oligonucleotide primers for inflammation and apoptosis-related genes and β-actin were designed using Primer 6.0 software (http://bioinfo.ut.ee/primer3-0.4.0/), based on the published GenBank sequences (Table 1; Niu et al., 2018a). qPCR was performed using the UltraSYBR Mixture (High ROX) (CWBIO, Beijing, China) and the ABI StepOne System (Applied Biosystems, Foster City, CA, USA). qPCR was conducted in a total volume of 20 μL, and the amplification steps consisted of 95°C for 10 min, followed by 40 cycles of denaturation at 95°C for 15 s and extension at 60°C for 1 min, followed by dissociation curve analysis. Each sample was analyzed in triplicate. Data were calculated based on the $2^{-\Delta\Delta}$Ct method. Relative mRNA expression was normalized to that of β-actin.

Statistical Analysis

All data are expressed as the mean ± standard deviation (SD). Statistical comparisons were analyzed by independent-sample t-tests and one-way analysis of variance using SPSS Statistics for Windows, version 20 (SPSS Inc., Chicago, IL, USA). $P < 0.05$ was considered statistically significant.

RESULTS

Influence of Infection FAdV-4 on Immune Organs

Statistical analyses revealed markedly lower immune organ-to-body weight (thymus and bursa) (Figure 1A and C) and higher spleen–body weight (Figure 1B) in the FAdV-4 group relative to the control group at 7 and 14 dpi ($P < 0.05$). However, no significant differences were evident at 21 dpi. Gross pathological analyses

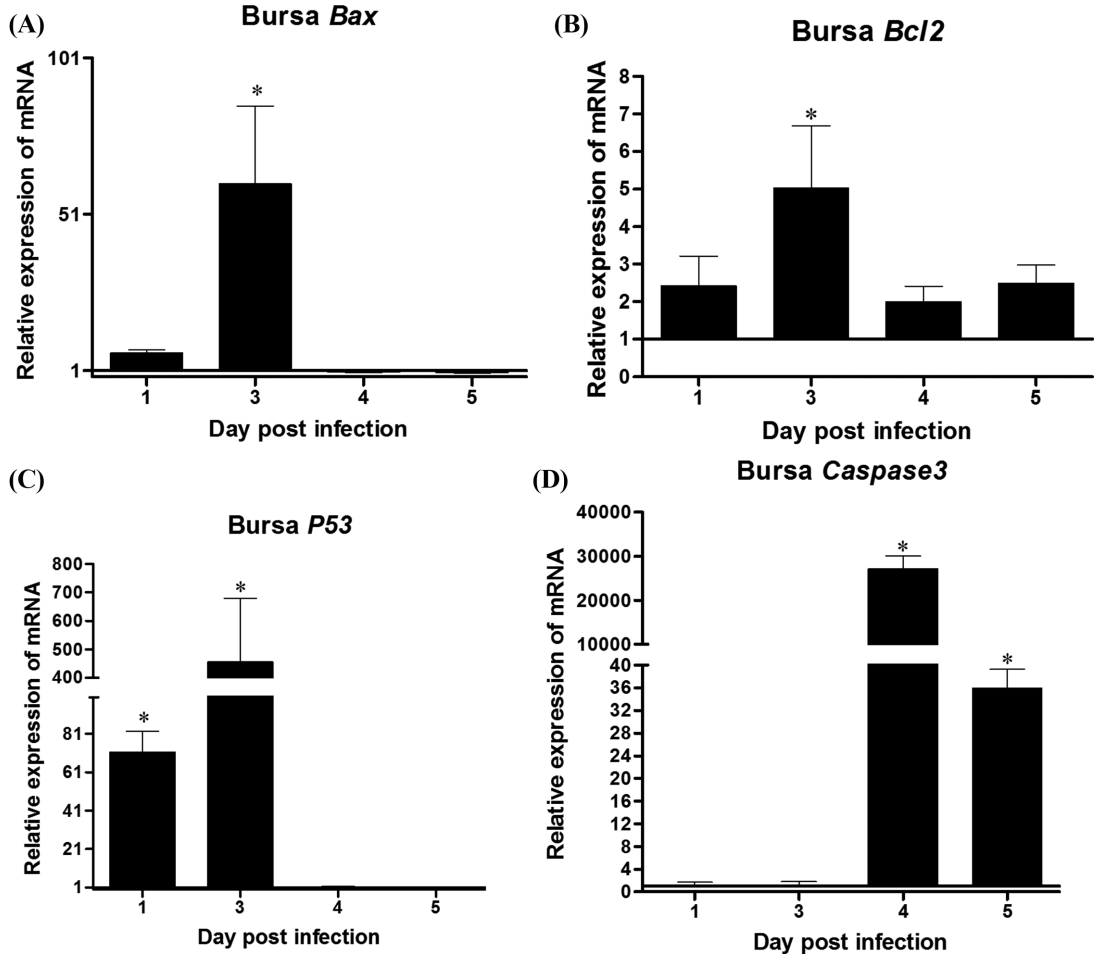

Figure 7. Expression profiles of apoptosis-related genes in the bursa at 1, 3, 4, and 5 d post-infection with fowl adenovirus serotype 4 infection. (A) *Bax,* (B) *Bcl2,* (C) *P53*, (D) *Caspase3* mRNA levels. The *y* axis represents the fold change in target gene expression in bursa compared with that of the control and the above line ($y = 1$) on the *x* axis represents the control. Data are expressed as mean ± SD ($n = 5$ chicken per group). Asterisks indicate significant differences ($P < 0.05$, by 1-way ANOVA).

disclosed enlarged spleen in FAdV-4 chickens with greater edema and congestion, compared with control chickens. The wet-to-dry weight ratio in spleen of chickens from the FAdV-4 group was significantly higher, compared to that in the control group at 5 to 14 dpi (Figure 1E). However, the wet-to-dry weight ratio in the thymus and bursa of the FAdV-4 group showed no significant differences relative to the control group (Figure 1D and F). Viral load in the thymus, spleen, and bursa of chickens showed similar trends, with a gradual increase at 1 to 7 dpi and a subsequent gradual decrease at 14 to 21 dpi. Notably, significant differences in viral load, compared spleen with thymus and bursa, were observed at 3 to 7 dpi ($P < 0.05$), while viral load was comparable between thymus and bursa (Figure 1G).

In histological sections of the bursa and thymus at 3 to 5 d after infection (Figure 2), the FAdV-4 group presented lymphocyte depletion in the medullary area of the bursa of Fabricius and thymus and interstitial edema in thymus. Necrosis of lymphocytes in the cortex of spleen was observed at 3 to 5 dpi.

Influence of FAdV Infection on HI Antibody Titers to NDV and AIV-H9 After Vaccination

As shown in Figure 3, humoral immune responses against inactivated NDV and AIV-H9 vaccine of the FAdV-4 plus vaccination group were similar to those of the vaccination group on day 7 after immunization ($P > 0.05$). Notably, the vaccination group exhibited significantly higher titers of NDV and AIV-H9 relative to the FAdV-4 plus vaccination group (1.65- and 1.67-fold, respectively), on day 14 after immunization ($P < 0.05$).

Apoptosis of Immune Organ

To ascertain whether FAdV-4 is involved in immune organs apoptosis, we performed a series of experiments. The brown spots observed with digoxigenin labeling indicated apoptotic cells. TUNEL staining revealed significant lymphocyte apoptosis in the FAdV-4 group, compared with the control group, at 5 dpi (Figure 4). *Bax*, *Bcl-2*, *P53,* and *Caspase-3* mRNA expression in

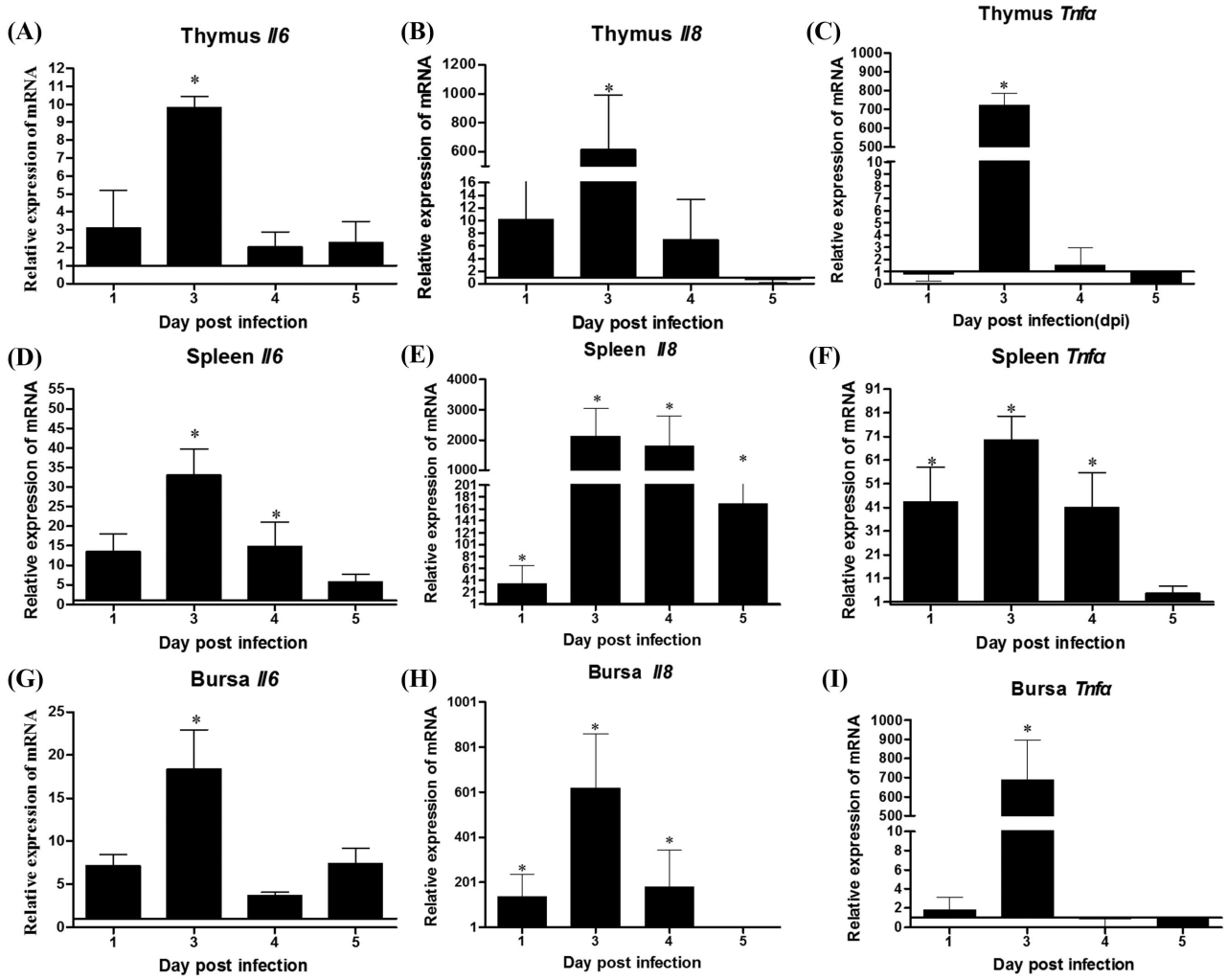

Figure 8. Expression profiles of inflammation-related genes in the immune organs at 1, 3, 4, and 5 d post-infection with fowl adenovirus serotype 4 infection. (A) *Il6,* (B) *Il8,* (C) *Tnfα* mRNA levels of thymus. (D) *Il6,* (E) *Il8,* (F) *Tnfα* mRNA levels of spleen. (G) *Il6,* (H) *Il8,* (I) *Tnfα* mRNA levels of bursa. The *y* axis represents the fold change in target gene expression in heart compared with that of the control and the above line ($y = 1$) on the *x* axis represents the control. Data are expressed as mean ± SD ($n = 5$ chicken per group). Asterisks indicate significant differences ($P < 0.05$, by 1-way ANOVA).

infected immune organs was additionally examined. In immune organs of the FAdV-4 group, *Bax*, *Bcl-2*, *P53*, and *Caspase-3* mRNA patterns showed similar significantly increasing trends at different time points, compared with the control group ($P < 0.05$, Figures 5–7). In thymus, *Bax* and *Bcl-2* levels were markedly upregulated by 736.43- and 4.56-fold, respectively, at 3 dpi. ($P < 0.05$, Figure 5A and B). Additionally, *P53* expression was significantly increased by 430.55- and 60.94-fold at 3 and 4 dpi, respectively ($P < 0.05$, Figure 5C). At 4 dpi, *Caspase-3* mRNA was enhanced up to 10.51-fold ($P < 0.05$, Figure 5D). In spleen, *Bax* and *Bcl-2* mRNA levels were 168.74- and 14.64-fold increased ($P < 0.05$, Figure 6A and B) and *P53* levels were 74.5- and 42.87-fold increased at 3 and 4 dpi ($P < 0.05$, Figure 6C), respectively. *Caspase-3* mRNA expression was significantly elevated, reaching 23.36- and 33.14-fold at 3 and 4 dpi, respectively ($P < 0.05$, Figure 6D). In bursa of Fabricius, *Bax* and *Bcl 2* levels were 60.76- and 5.02-fold increased, respectively, at 3 dpi ($P < 0.05$, Figure 7A and B). *P53* mRNA levels were markedly upregulated by 71.52- and 454.7-fold at 1 and 3 dpi ($P < 0.05$, Figure 7C) and *Caspase-3* mRNA by 27065.4- and 35.93-fold at 4 and 5 dpi ($P < 0.05$, Figure 7D), respectively.

Inflammation of Immune Organ

The mRNA expression of cytokines after inoculating chickens with FAdV-4 was measured in immune organs at 1, 3, 4, and 5 dpi. Transcription of inflammatory cytokines (*Il6, Il8*, and *Tnfα*) was all upregulated in the immune organs of FAdV-4-treated chickens at various time points to a significantly different extent relative to the control ($P < 0.05$, Figure 8). As shown in Figures 8A–C, relative to the control group, *Il6, Il8*, and *Tnfα* mRNA levels in thymus were significantly upregulated by 9.8-, 616.51- and 720.03-fold at 3 dpi, respectively. In spleen, *Il6* showed a marked increase in expression, reaching 33.12- and 14.75-fold at

3 and 4 dpi, respectively ($P < 0.05$, Figure 8D). Moreover, *Il8* mRNA expression was upregulated (36.19-, 2124.06-, 1817.91-, and 170.07-fold at 1, 3, 4, and 5 dpi, respectively; $P < 0.05$) (Figure 8E), along with *Tnfα* (43.48-, 69.73-, and 41.06-fold, respectively; $P < 0.05$) (Figure 8F). In bursa of Fabricius, *Il6* and *Tnfα* mRNA levels were significantly increased by 18.43- and 689.27-fold, respectively, at 3 dpi ($P < 0.05$, Figure 8G and I). And *Il8* showed elevated expression at 1, 3, and 4 dpi (136.32-, 617.63- and 178.69-fold, respectively; $P < 0.05$) (Figure 8H).

DISCUSSION

FAdV-4 is the known etiological agent of HPS (Ganesh and Raghavan, 2000). HPS caused by FAdV-4 follows an unusually aggressive clinical course, ranging from 7 to 500 d, and different varieties of chickens share similar sensitivities to FAdV-4 under field conditions (Anjum et al., 1989; Niu et al., 2017). Several reports have showed that virulent FAdV-4 strains have high pathogenicity to embryos and SPF chickens (Li et al., 2016, 2017). Long-term surveillance of FAdV-4 in China revealed common co-infection with different immunosuppressive viruses in HPS cases, such as chicken infectious anemia virus, Marek's disease virus, and reticuloendotheliosis virus (Li et al., 2016; Niu et al., 2017; Meng et al., 2018). However, limited evidence has been recorded regarding the presence of HPS-associated adenovirus in the lymphoid organs or its involvement as an immunosuppressive agent.

In the present study, the morphology of lymphoid organs in experimentally infected chicks was examined. The results indicated that the FAdV-4 strain triggered depletion of lymphocytes and growth impairment in thymus and bursa. Interestingly, spleen–body weight and wet-dry weight ratios in spleen of the FAdV-4 group were significantly higher than those of the control group. Necrosis of lymphocytes in the cortex of spleen was observed at 3 to 5 dpi. Theoretically, the spleen is rich in blood and congestion is often observed under conditions of heart failure (Mebius and Kraal, 2005). Therefore, formation of pericardial effusion is speculated to splenic congestion, and the organ index consequently becomes larger. Viral loads were consistent in the lymphoid organs but remained high in spleen. Further investigations focusing on viral location in these organs should aid in determining the level of damage.

Our experiments additionally showed that chickens infected with FAdV-4 experienced greater inhibition of antibody responses to inactivated vaccines against ND and AIV-H9, compared to chickens in the vaccination group (Figure 3). Along with histopathological changes to lymphoid organs, FAdV-4 infection caused suppression of the humoral immune response. The mechanisms underlying adenovirus-mediated lymphoid organ damage were further investigated using TUNEL and apoptotic gene transcription analyses. Lymphocyte apoptosis in lymphoid organs was evident at 5 dpi (Figure 4). Further evidence of apoptosis was obtained based on expression patterns of apoptosis-associated genes (*Bax*, *Bcl2*, *P53*, and *Caspase-3*) (Nkpaa et al., 2018). As expected, *Caspase-3* mRNA was significantly upregulated at 4 to 5 dpi in 3 organs. Caspase proteins play important roles in the decisive stage of apoptosis (Belmokhtar et al., 2011). In the majority of apoptosis-inducing processes, transcriptional levels of caspases are significantly increased. Caspase-3 is an important effector molecule in the caspase cascade activation that, once activated, triggers characteristic apoptotic changes in cells (Green, 1998; Thomberry and Littlewood, 1998; Rogers et al., 2017). In our experiments, pro-apoptotic *Bax* and *P53* genes were significantly increased at different time points in the 3 lymphoid organs (Wei et al., 2016). Interestingly, *Bcl2*, an inhibitor of apoptotic genes, was also upregulated at 3, 4, and 3 dpi in thymus, spleen, and brusa, respectively. However, Bax and Bcl-2 combine to form a heterodimer, which leads to loss of the inhibitory effect of Bcl-2 on apoptosis (Qin et al., 2015; Kvansakul et al., 2017). Preliminary data suggested that FAdV-4 induced lymphocyte apoptosis, which would promote lymph organ damage. However, the specific apoptotic pathways and mechanisms remain to be elucidated.

To determine the mechanisms underlying the inflammatory response of immune organs following FAdV-4 infection, mRNA expression of 4 cytokines (IL-6, IL-8, and TNF-α) was assessed. Western blot analyses to assess protein expression should be conducted to further support these findings. However, commercial poultry antibodies were not easily available and ELISA kits were not sufficiently sensitive in detecting specific cytokine contents in poultry tissue. Therefore, mRNA measurement presents a good alternative to detect transcriptional levels in the absence of available poultry antibodies. These cytokines are considered the most important signaling molecules in the induction and regulation of the inflammatory response (Laurent et al., 2001; Chen et al., 2009; Sanchez et al., 2011). Increased transcription of inflammatory factors promotes inflammation, further inducing accumulation of various inflammatory cells and release of several soluble inflammatory regulators, reactive oxygen species, lipid regulators, proteases and cytokines, and subsequent tissue damage (Bhargava et al., 2013; Mirantes et al., 2014; Pourgholaminejad et al., 2016).

CONCLUSION

Data from our systematic examination of FAdV-4-induced damage to the structure and function of immune organs indicated that FAdV-4 triggered apoptosis and a severe inflammatory response. Further exploration of the molecular basis of FAdV-4-mediated apoptosis and inflammatory responses is essential to clarify the overall pathologic mechanisms of adenovirus-induced disease.

ACKNOWLEDGMENTS

This study was supported by the Qingdao talent plan and Funds of Shandong "Double Tops" Program.

REFERENCES

Anjum, A., M. Sabri, and Z. Iqbal. 1989. Hydropericarditis syndrome in broiler chickens in Pakistan. PLoS One 12:1312–1316.

Barlan, A. U., T. M. Griffin, K. A. Mcguire, and C. M. Wiethoff. 2011. Adenovirus membrane penetration activates the nlrp3 inflammasome. J. Virol. 85:146–155.

Belmokhtar, C. A., J. Hillion, and E. Ségal-Bendirdjian. 2011. Staurosporine induces apoptosis through both caspase-dependent and caspase-independent mechanisms. Oncogene 20:3354–3362.

Bhargava, R., W. Janssen, C. Altmann, A. Andrés-Hernando, K. Okamura, R. Vandivier, N. Ahuja, and S. Faubel. 2013. Intratracheal IL-6 protects against lung inflammation in direct, but not indirect, causes of acute lung injury in mice. PLoS One 8:e61405.

Chen, L., M. J. Ran, X. Shan, M. Cao, P. Cao, X. Yang, and S. Zhang. 2009. Baff enhances b-cell-mediated immune response and vaccine-protection against a very virulent IBDV in chickens. Vaccine 27:1393–1399.

Choi, K. S., S. J. Kye, J. Y. Kim, W. J. Jeon, E. K. Lee, K. Y. Park, and H. W. Sung. 2012. Epidemiological investigation of outbreaks of fowl adenovirus infection in commercial chickens in Korea. Poult Sci. 91:2502–2506.

Ganesh, K., and R. Raghavan. 2000. Hydropericardium hepatitis syndrome of broiler poultry:current status of research. Res. Vet. Sci. 68:201–206.

Green, D. R. 1998. Apoptotic pathways: the roads to ruin. Cell 94:695–698.

Jiang, H., E. J. White, C. I. Ríosvicil, J. Xu, C. Gomezmanzano, and J. Fueyo. 2011. Human adenovirus type 5 induces cell lysis through autophagy and autophagy-triggered caspase activity. J. Virol. 85:4720–4729.

Kaján, G. L., S. Kecskeméti, B. Harrach, and M. Benkő. 2013. Molecular typing of fowl adenoviruses, isolated in Hungary recently, reveals high diversity. Vet. Microbiol. 167:357.

Kawai, T., and S. Akira. 2008. Toll-like receptor and RIG-I-like receptor signaling. Ann. NY Acad. Sci. 1143:1–20.

Kvansakul, M., S. Caria, and M. G. Hinds. 2017. The Bcl-2 family in host-virus interactions. Viruses 9:290.

Laurent, F., R. Mancassola, S. Lacroix, R. Menezes, and M. Naciri. 2001. Analysis of chicken mucosal immune response to Eimeria tenella and Eimeria maxima infection by quantitative reverse transcription-PCR. Infect. Immun. 69:2527–2534.

Levine, B. 2005. Eating oneself and uninvited guests: autophagy-related pathways in cellular defense. Cell 120:159–162.

Li, H., J. Wang, L. Qiu, Z. Han, and S. Liu. 2016. Fowl adenovirus species C serotype 4 is attributed to the emergence of hepatitis-hydropericardium syndrome in chickens in China. Infect. Genet. Evol. 45:230–241.

Li, P. H., P. P. Zheng, T. F. Zhang, G. Y. Wen, H. B. Shao, and Q. P. Luo. 2017. Fowl adenovirus serotype 4: Epidemiology, pathogenesis, diagnostic detection, and vaccine strategies. Poult. Sci. 96:2630–2640.

Lobanov, V. A., V. V. Borisov, A. V. Borisov, V. V. Drygin, A. A. Gusev, M. M. Shmarov, T. A. Akopian, and B. S. Naroditskii. 2000. Sequence analysis of hexon gene from adenovirus KR95 inducing hydropericardium syndrome in chickens. Mol. Gen. Mikrobiol. Virusol. 1:30–36.

Manicassamy, S., and B. Pulendran. 2009. Modulation of adaptive immunity with Toll-like receptors. Semin. Immunol. 21:185–193.

Mebius, R. E., and G. Kraal 2005. Structure and function of the spleen. Nat. Rev. Immunol. 5:606–616.

Meng, F., G. Dong, Y. Zhang, S. Tian, Z. Cui, S. Chang, and P. Zhao. 2018. Co-infection of fowl adenovirus with different immunosuppressive viruses in a chicken flock. Poult. Sci. 97:1699–1705.

Mirantes, C., E. Passegué, and E. M. Pietras. 2014. Pro-inflammatory cytokines: emerging players regulating hsc function in normal and diseased hematopoiesis. Exp. Cell Res. 329:248–254.

Niu, Y. J., Q. Q. Sun, X. P. Liu, and S. D. Liu. 2018a. Mechanism of fowl adenovirus serotype 4-induced heart damage and formation of pericardial effusion. Poult. Sci. doi: 10.3382/ps/pey485.

Niu, Y. J., Q. Q. Sun, G. H. Zhang, W. Sun, X. P. Liu, Y. L. Shang, Y. H. Xiao, and S. D. Liu. 2018b. Fowl adenovirus serotype 4-induced apoptosis, autophagy, and a severe inflammatory response in liver. Vet. Microbiol. 223:34–41.

Niu, Y. J., Q. Q. Sun, G. H. Zhang, W. Sun, X. P. Liu, Y. L. Shang, Y. H. Xiao, and S. D. Liu. 2017. Epidemiological investigation of outbreaks of fowl adenovirus infections in commercial chickens in China. Transbound. Emerg. Dis. 65:e121–e126.

Niu, Y. J., W. Sun, G. H. Zhang, Y. J. Qu, P. F. Wang, H. L. Sun, L. Y. Wang, Y. H. Xiao, and S. D. Liu. 2016. Hydropericardium syndrome outbreak caused by fowl adenovirus serotype 4 in China in 2015. J. Gen. Virol. 97:2684–2690.

Nkpaa, K. W., I. O. Awogbindin, B. A. Amadi, A. O. Abolaji, I. A. Adedara, M. O. Wegwu, and E. O. Farombi. 2018. Ethanol exacerbates manganese-induced neurobehavioral deficits, striatal oxidative stress, and apoptosis via regulation of p53, caspase-3, and bax/bcl-2 ratio-dependent pathway. Biol. Trace Elem. Res. doi: 10.1007/s12011-018-1587-4.

Ojkic, D., E. Martin, J. Swinton, J. Vaillancourt, M. Boulianne, and S. Gomis. 2008. Genotyping of Canadian isolates of fowl adenoviruses. Avian Pathol. 37:95–100.

Pourgholaminejad, A., N. Aghdami, H. Baharvand, and S. M. Moazzeni. 2016. The effect of pro-inflammatory cytokines on immunophenotype, differentiation capacity and immunomodulatory functions of human mesenchymal stem cells. Cytokine 85:51–60.

Pruijssers, A., H. Hengel, T. Abel, and T. Dermody. 2013. Apoptosis induction influences reovirus replication and virulence in newborn mice. J. Virol. 87:12980–12989.

Qin, G., L. Wu, H. Liu, Y. Pang, C. Zhao, S. Wu, X. Wang, and T. Chen. 2015. Artesunate induces apoptosis via a ros-independent and bax-mediated intrinsic pathway in HepG2 cells. Exp. Cell Res. 33:308–317.

Radke, J., F. Grigera, D. Ucker, and J. Cook. 2014. Adenovirus E1B 19-kilodalton protein modulates innate immunity through apoptotic mimicry. J. Virol. 88:2658–2669.

Rodriguez-Rocha, H., J. Gomez-Gutierrez, A. Garcia-Garcia, X. Rao, L. Chen, K. Mcmasters, and H. S. Zhou. 2011. Adenoviruses induce autophagy to promote virus replication and oncolysis. Virology 416:9.

Rogers, C., T. Fernandes-Alnemri, L. Mayes, D. Alnemri, G. Cingolani, and E. S. Alnemri. 2017. Cleavage of dfna5 by caspase-3 during apoptosis mediates progression to secondary necrotic/pyroptotic cell death. Nat. Commun. 8:14128.

Ruan, S., J. Zhao, Z. He, H. Yang, and G. Zhang. 2018. Analysis of pathogenicity and immune efficacy of fowl adenovirus serotype 4 isolates. Poult Sci. 97:2647–2653.

Sanchez, R., P. González, S. Gómezpuerta, G. Noda, R. Vega, J. Águila-Benites, L. Suárez-Amarán, N. C. Parra, and J. R. Toledo-Alonso. 2011. Avian CD154 enhances humoral and cellular immune responses induced by an adenovirus vector-based vaccine in chickens. Comp. Immunol. Microbiol. Infect. Dis. 34:259–265.

Schachner, A., A. Marek, B. Jaskulska, I. Bilic, and M. Hess. 2014. Recombinant FAdV-4 fiber-2 protein protects chickens against hepatitis-hydropericardium syndrome (HHS). Vaccine 32:1086–1092.

Thomberry, N. A., and Y. Littlewood. 1998. Caspases: enemies within. Science 281:1312–1316.

Wei, Y., F. J. Yuan, W. B. Zhou, L. Wu, L. Chen, J. J. Wang, and Y. S. Zhang. 2016. Borax-induced apoptosis in HepG2 cells involves p53, bcl-2, and bax. Genet. Mol. Res. 15. doi: 10.4238/gmr.15028300.

Zhong, Y., Y. Liao, S. Fang, J. Tam, and D. Liu. 2012. Up-regulation of Mcl-1 and Bak by coronavirus infection of human, avian and animal cells modulates apoptosis and viral replication. PLoS One 7:e30191.